

Examining the Conditioning Factors that Influence Material Shear Strength of Particle Deposits in a Full-Scale Drinking Water Distribution Laboratory

Artur Sass Braga, Yves Filion

Supplementary Data

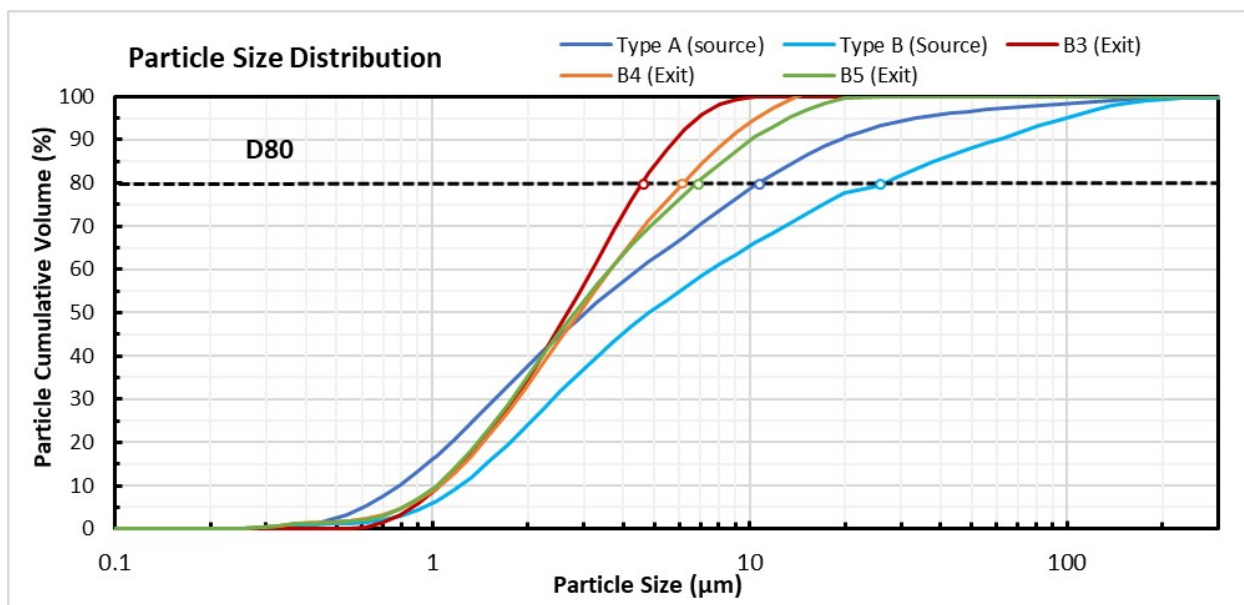


Figure S1. Particle size distribution of suspended particles collected among the experiments. D80 dashed line highlights the size where the particles cumulative volume achieves 80% of all particles identified in the sample. This size represents a comparable particle size metric among the different samples, and demonstrates that samples collected at the 'exit' of the pipes were typically smaller than particles introduced in the system as a 'source' at the start of the experiment.

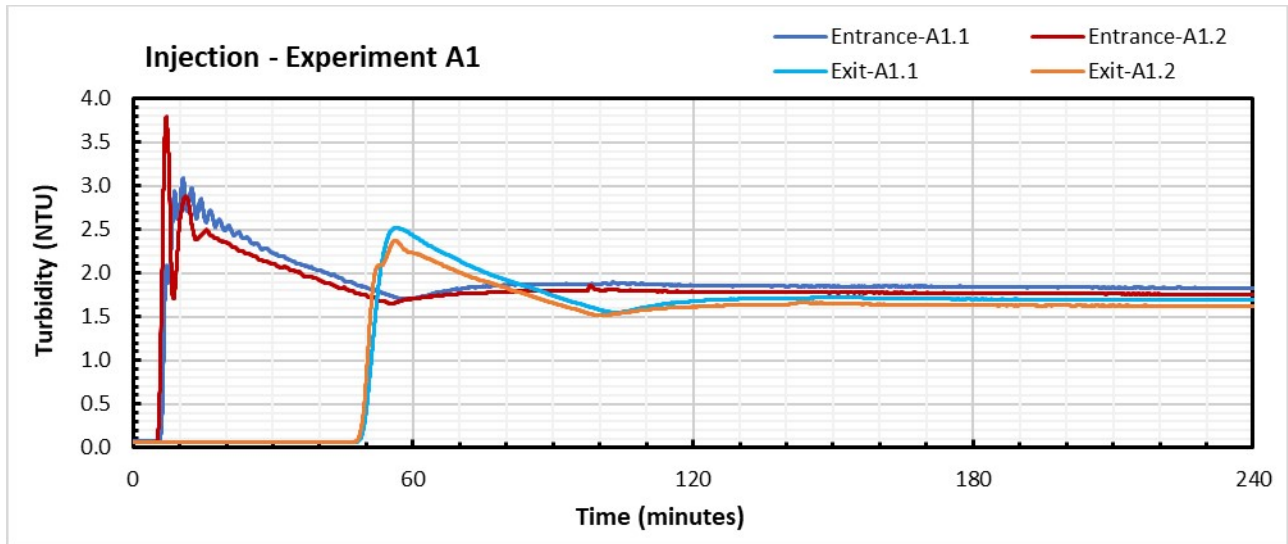


Figure S2. Turbidity profiles at the 'Entrance' and 'Exit' of the pipes of Experiments A1.1 and A1.2, after an instantaneous injection of the synthetic iron oxide particles into the tank of the system.

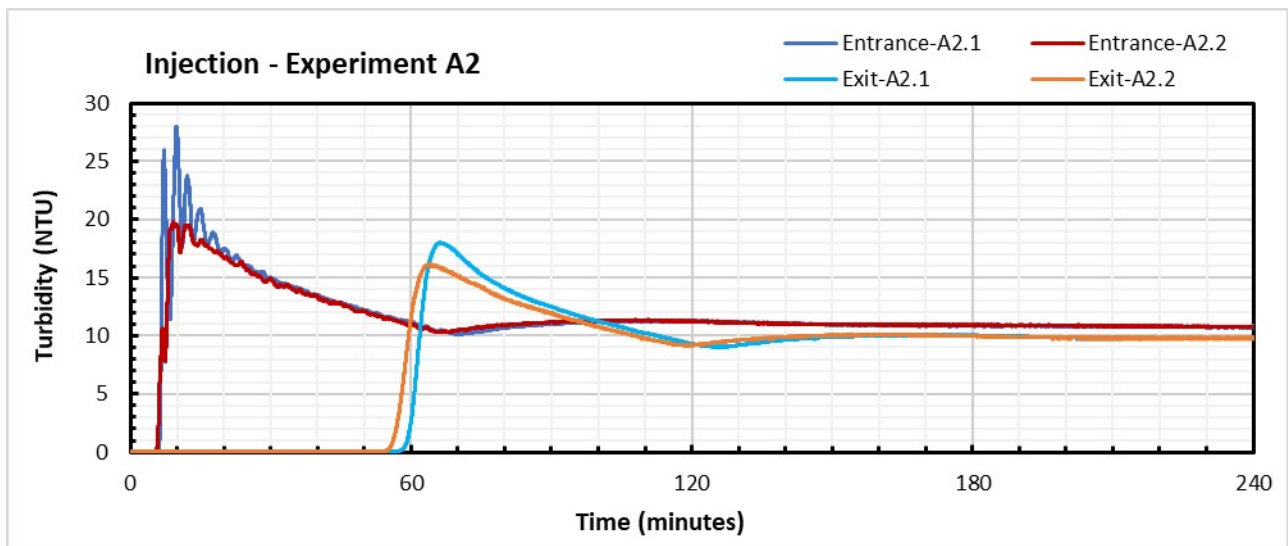


Figure S3. Turbidity profiles at the 'Entrance' and 'Exit' of the pipes of Experiments A2.1 and A2.2, after an instantaneous injection of the synthetic iron oxide particles into the tank of the system.

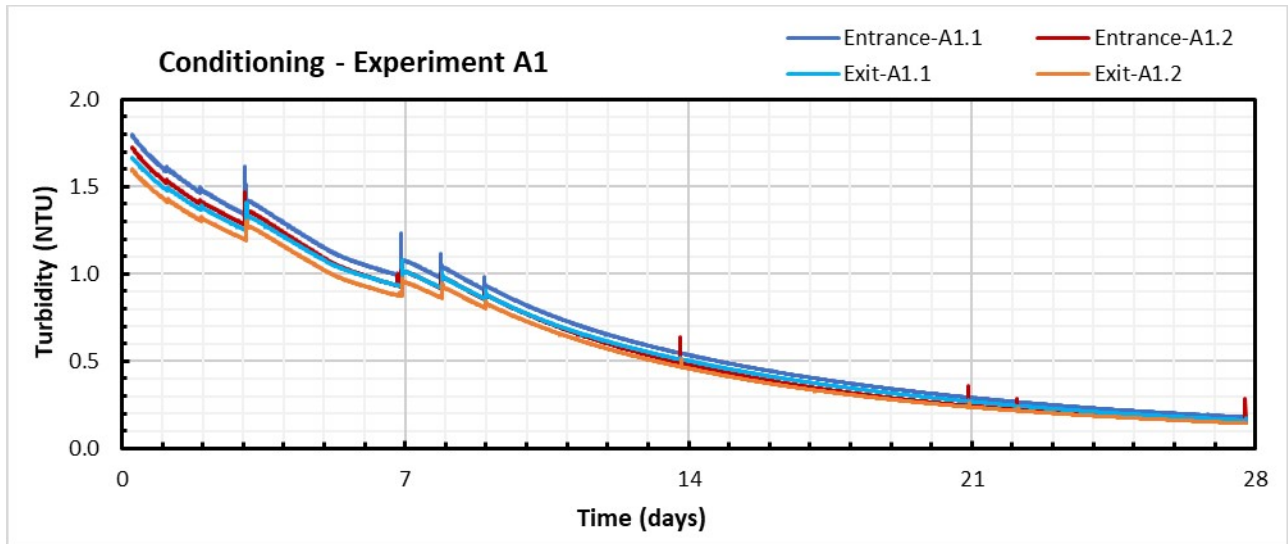


Figure S4. Turbidity profiles at the 'Entrance' and 'Exit' of the pipes of Experiments A1.1 and A1.2, during the 28 days conditioning period

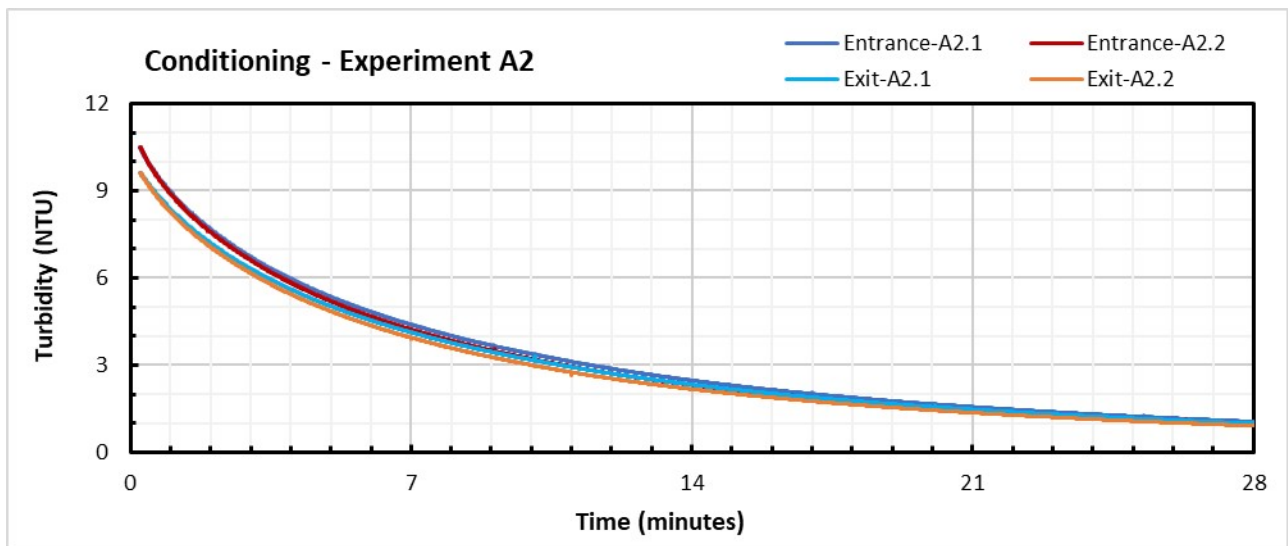


Figure S4. Turbidity profiles at the 'Entrance' and 'Exit' of the pipes of Experiments A2.1 and A2.2, during the 28 days conditioning period

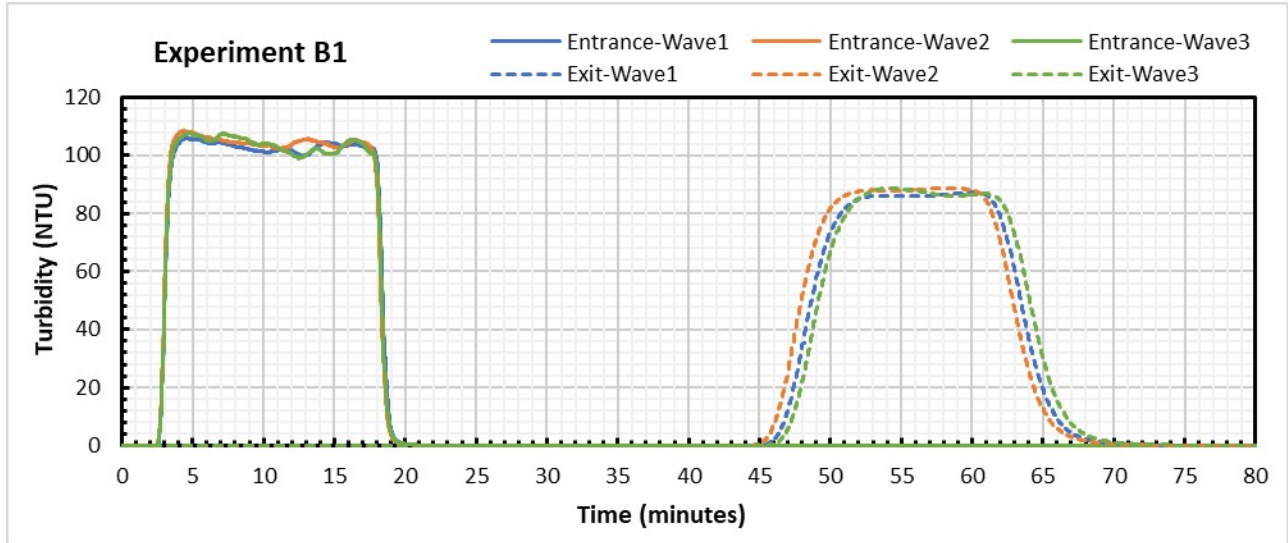


Figure S5. Turbidity profiles at the 'Entrance' and 'Exit' of the pipes of Experiment B1, during the passage of the 3 consecutive waves of high concentrated particles.

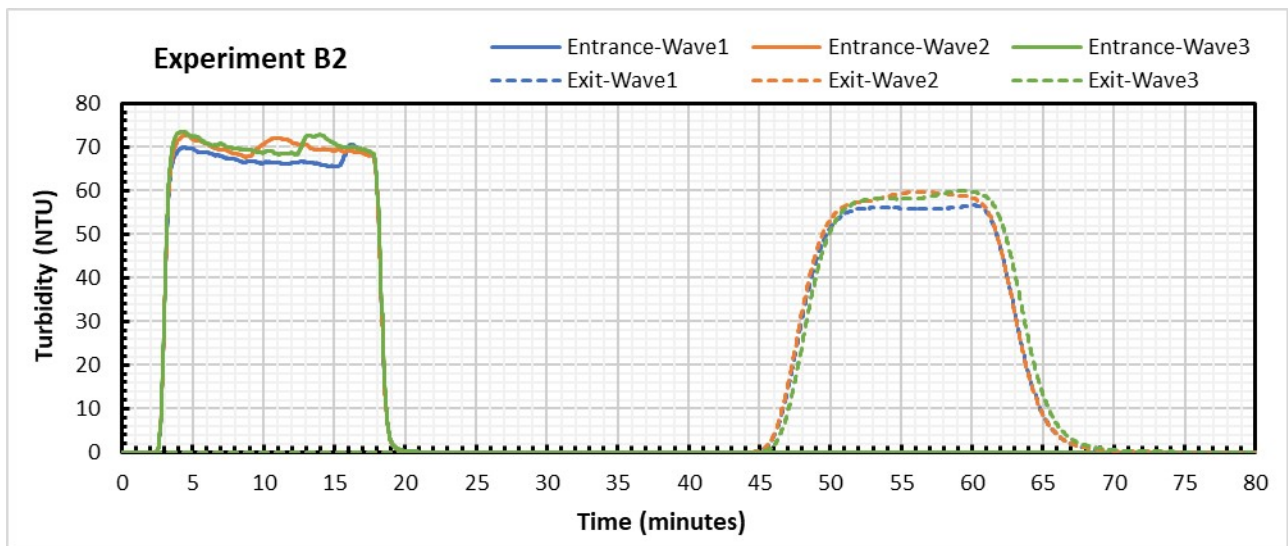


Figure S6. Turbidity profiles at the 'Entrance' and 'Exit' of the pipes of Experiment B2, during the passage of the 3 consecutive waves of high concentrated particles.

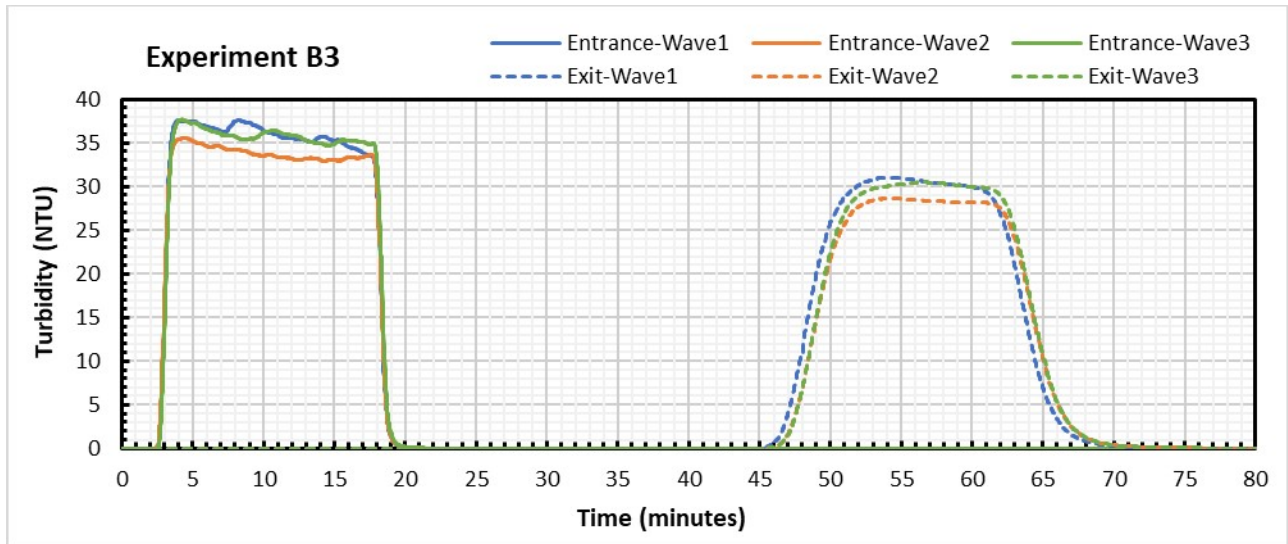


Figure S7. Turbidity profiles at the 'Entrance' and 'Exit' of the pipes of Experiment B3, during the passage of the 3 consecutive waves of high concentrated particles.

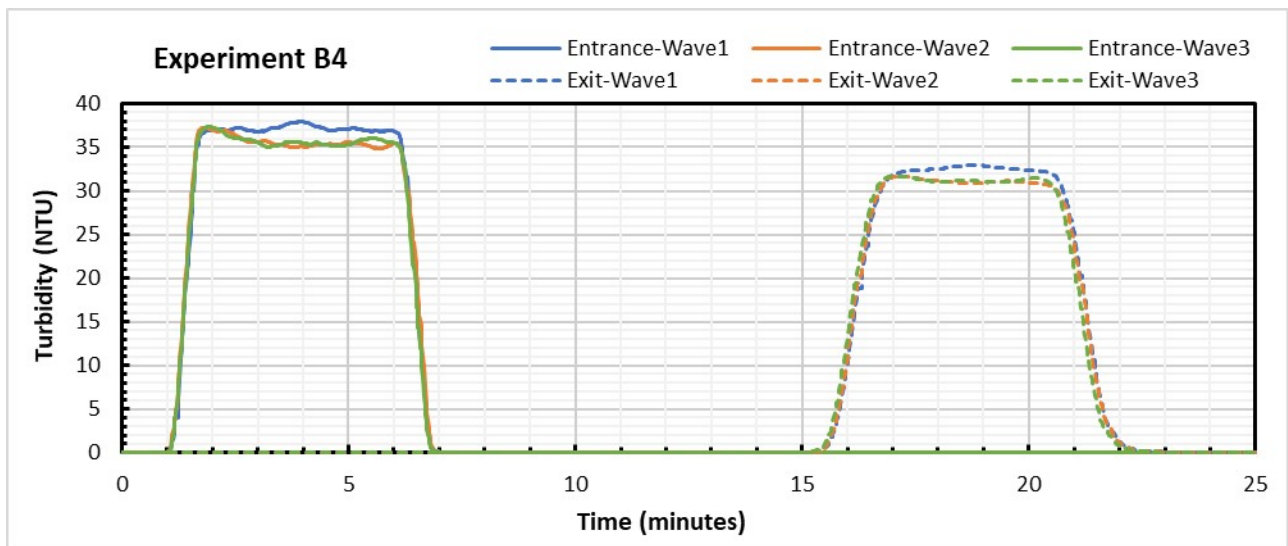


Figure S8. Turbidity profiles at the 'Entrance' and 'Exit' of the pipes of Experiment B4, during the passage of the 3 consecutive waves of high concentrated particles.

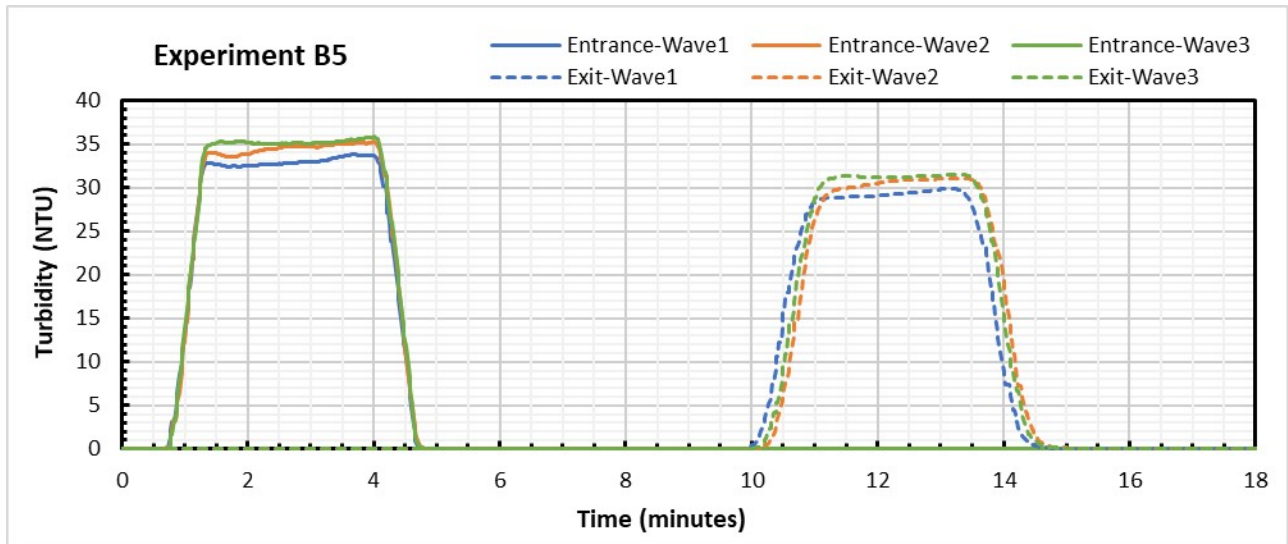


Figure S9. Turbidity profiles at the 'Entrance' and 'Exit' of the pipes of Experiment B5, during the passage of the 3 consecutive waves of high concentrated particles.

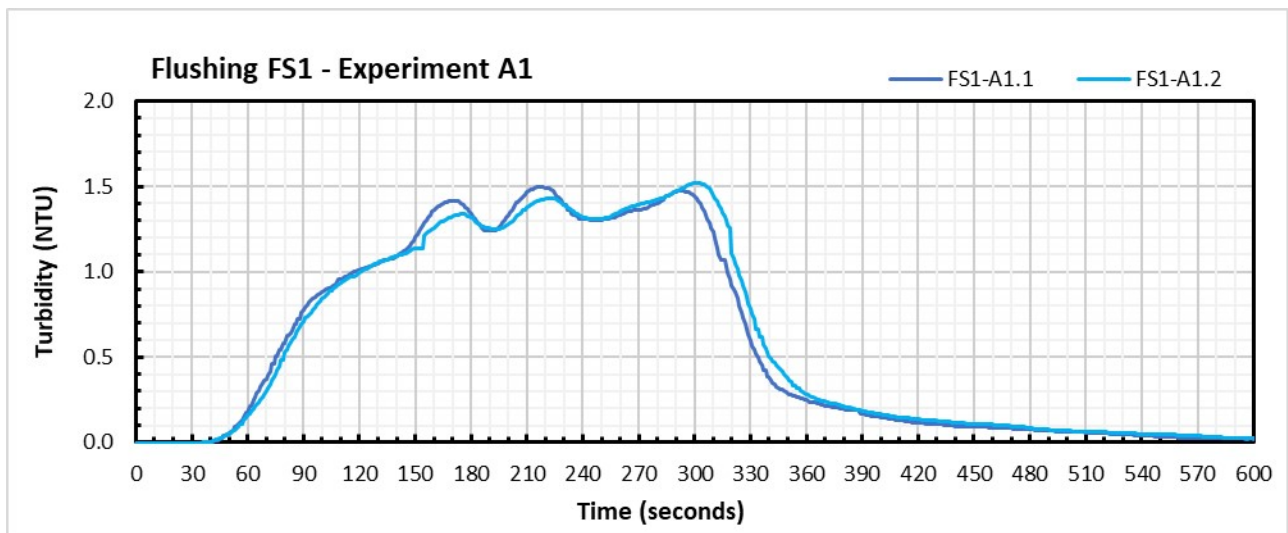


Figure S10. Turbidity profiles at the 'Exit' of the pipes of Experiments A1.1 and A1.2, during the first flushing step (FS1).

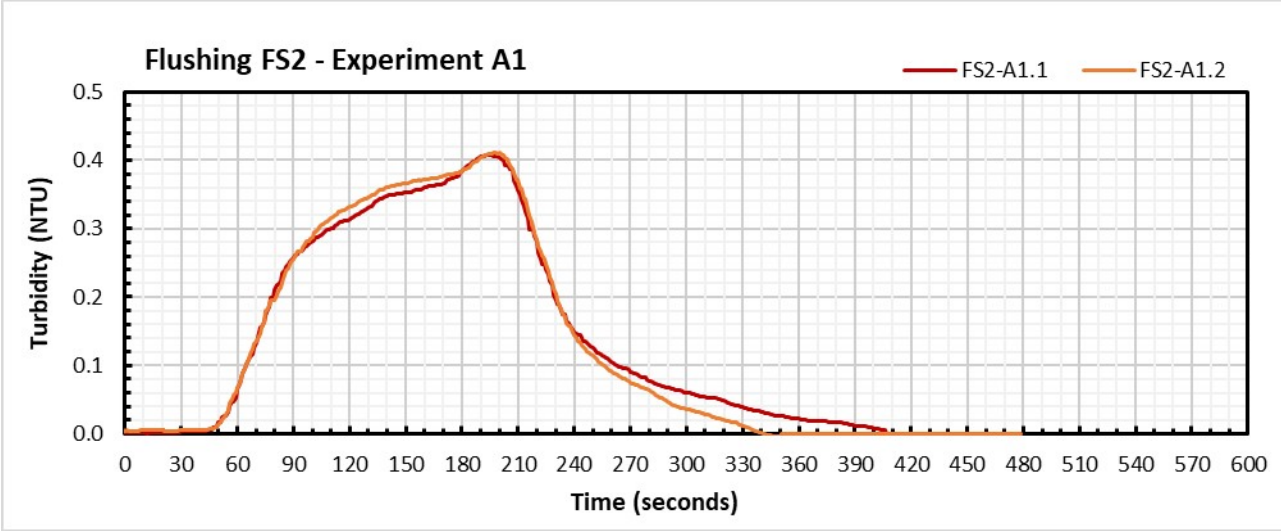


Figure S11. Turbidity profiles at the 'Exit' of the pipes of Experiments A1.1 and A1.2, during the second flushing step (FS2).

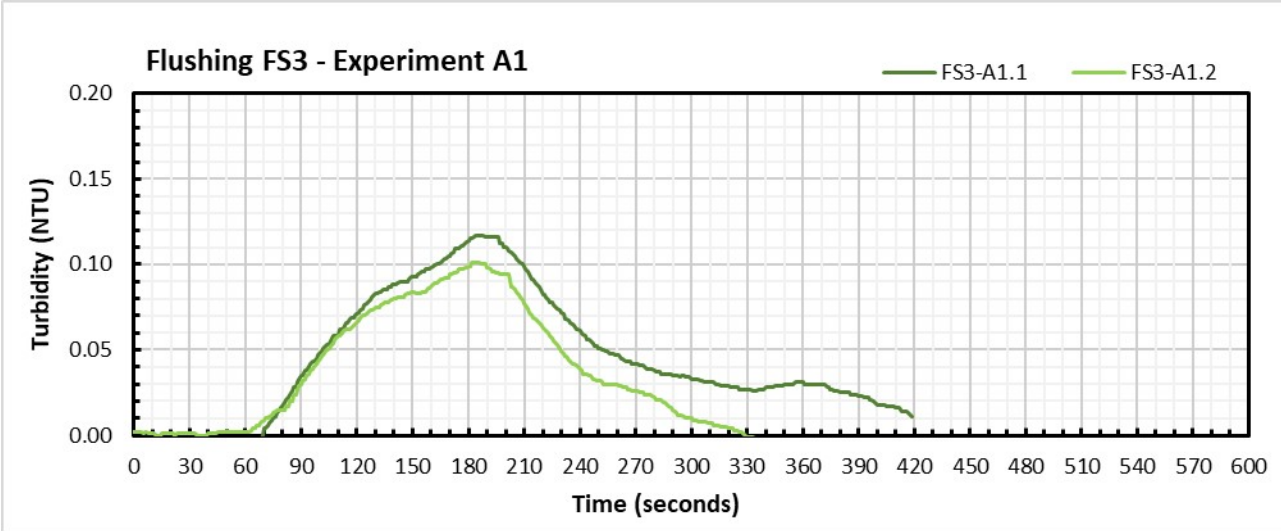


Figure S12. Turbidity profiles at the 'Exit' of the pipes of Experiments A1.1 and A1.2, during the third flushing step (FS3).

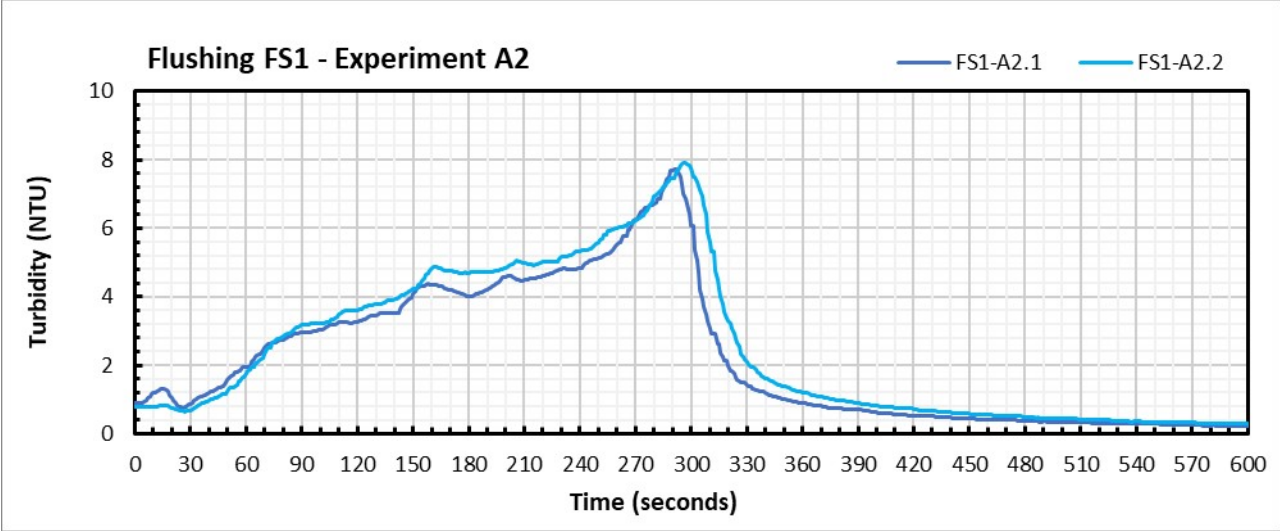


Figure S13. Turbidity profiles at the 'Exit' of the pipes of Experiments A2.1 and A2.2, during the first flushing step (FS1).

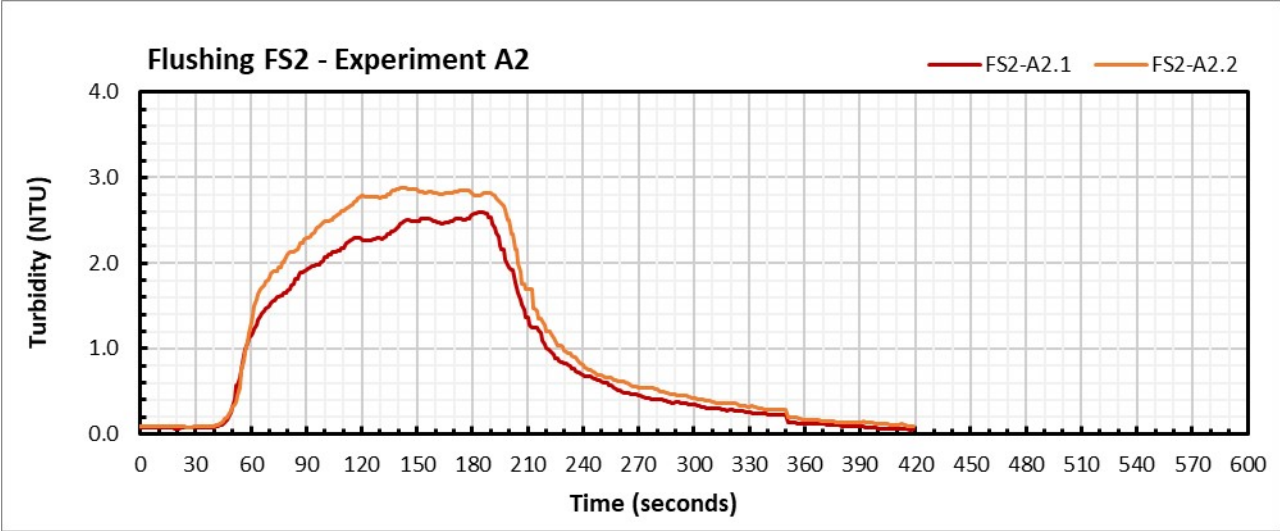


Figure S14. Turbidity profiles at the 'Exit' of the pipes of Experiments A2.1 and A2.2, during the second flushing step (FS2).

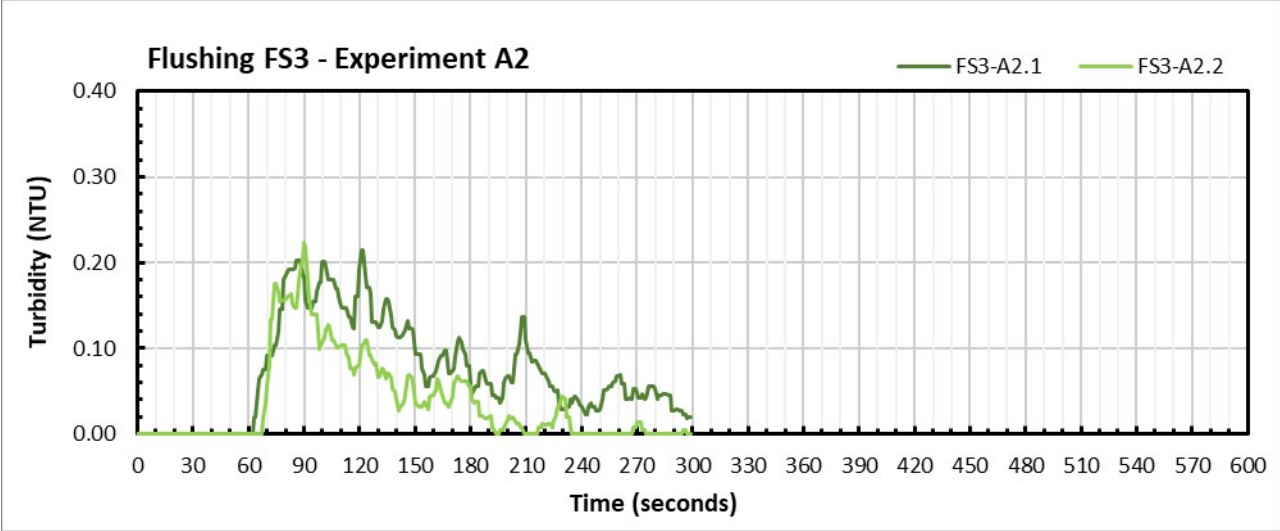


Figure S15. Turbidity profiles at the 'Exit' of the pipes of Experiments A2.1 and A2.2, during the third flushing step (FS3).

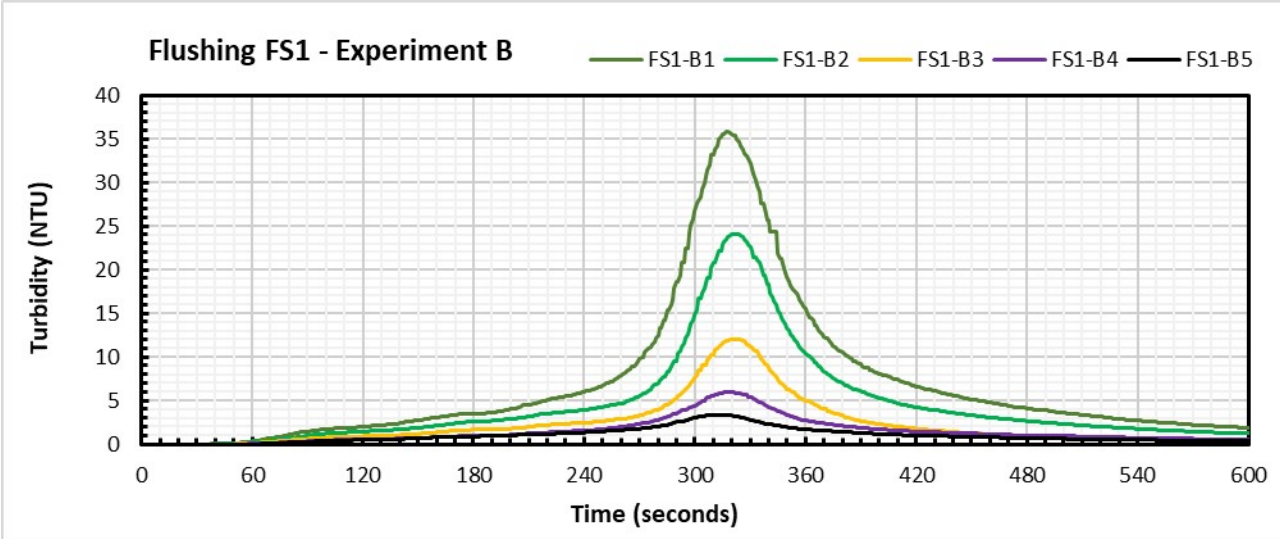


Figure S16. Turbidity profiles at the 'Exit' of the pipes of Experiments Type B, during the first flushing step (FS1).

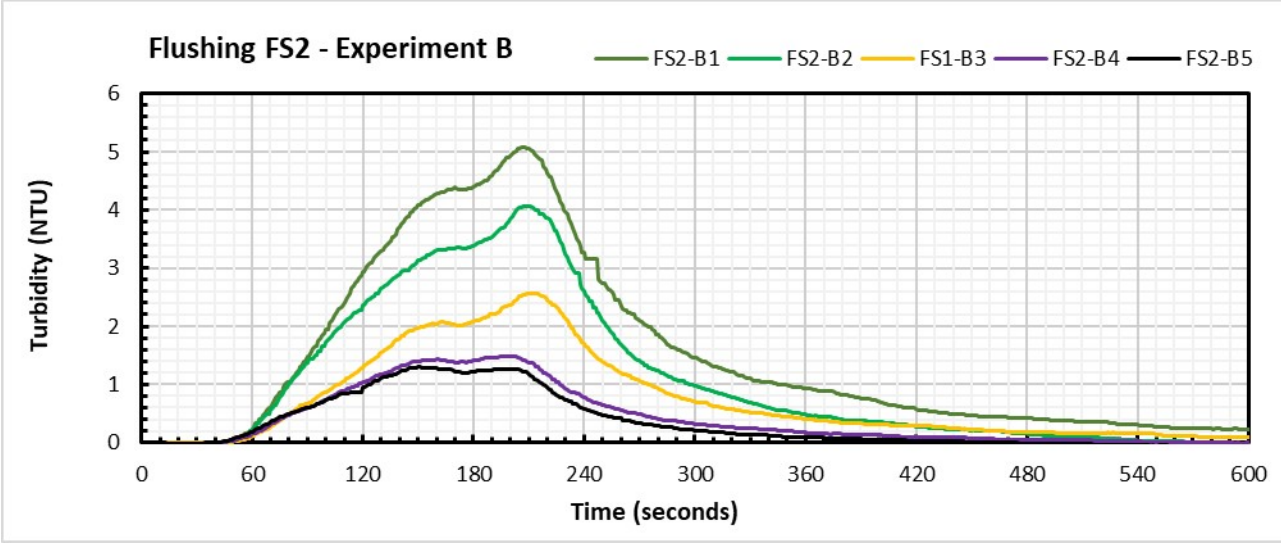


Figure S17. Turbidity profiles at the 'Exit' of the pipes of Experiments Type B, during the second flushing step (FS2).

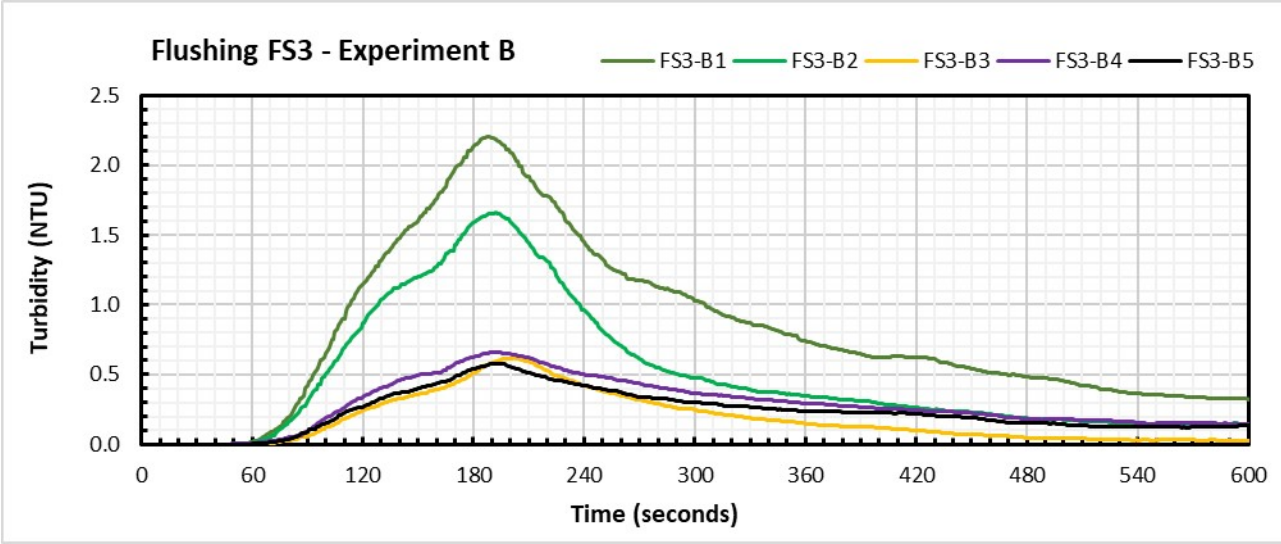


Figure S18. Turbidity profiles at the 'Exit' of the pipes of Experiments Type B, during the third flushing step (FS3).

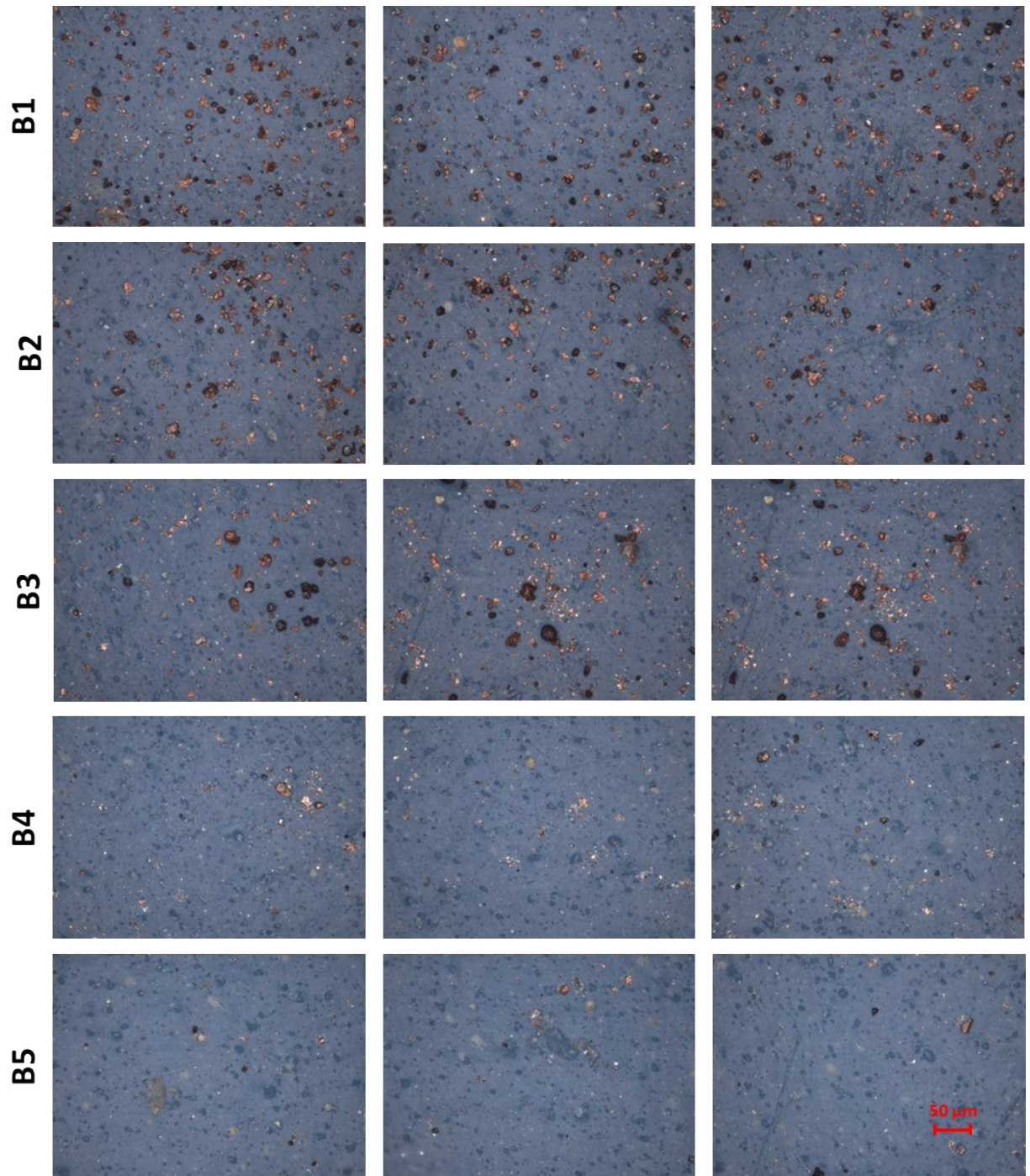


Figure S19. Brightfield microscopy images of three randomly selected fields of views from samples collected at the end of the conditioning phase of Experiments Type B. Images from experiments realized with larger particle concentration (B1 and B2) and lower conditioning velocities (B1, B2, B3) have larger and more abundant particles. Particles of experiments B4 and B5, realized at higher velocities, are sparse and consistently smaller in size.



Figure S20. Brightfield microscopy images of three randomly selected fields of views from samples collected after the first (FS1), second (FS2) and third (FS3) flushing steps of the Experiment B1, realized with the larger concentration of suspended particles and lower water velocity. The images highlight that the larger particles previously observed prior flushing (Figure S21) are no longer present in the pipes, and a substantial decrease of particles size and abundance occurred for each sequential flushing step.

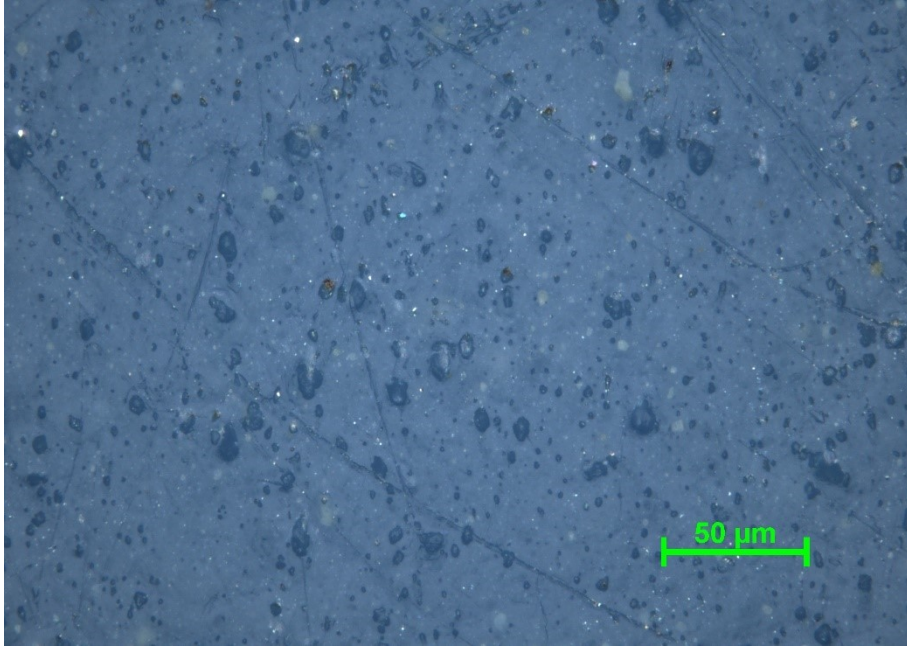


Figure S21. Brightfield microscopy image of a clean PVC pipe sample cut directly from a raw pipe used for municipal pipe mains, realized at magnification of 400X.

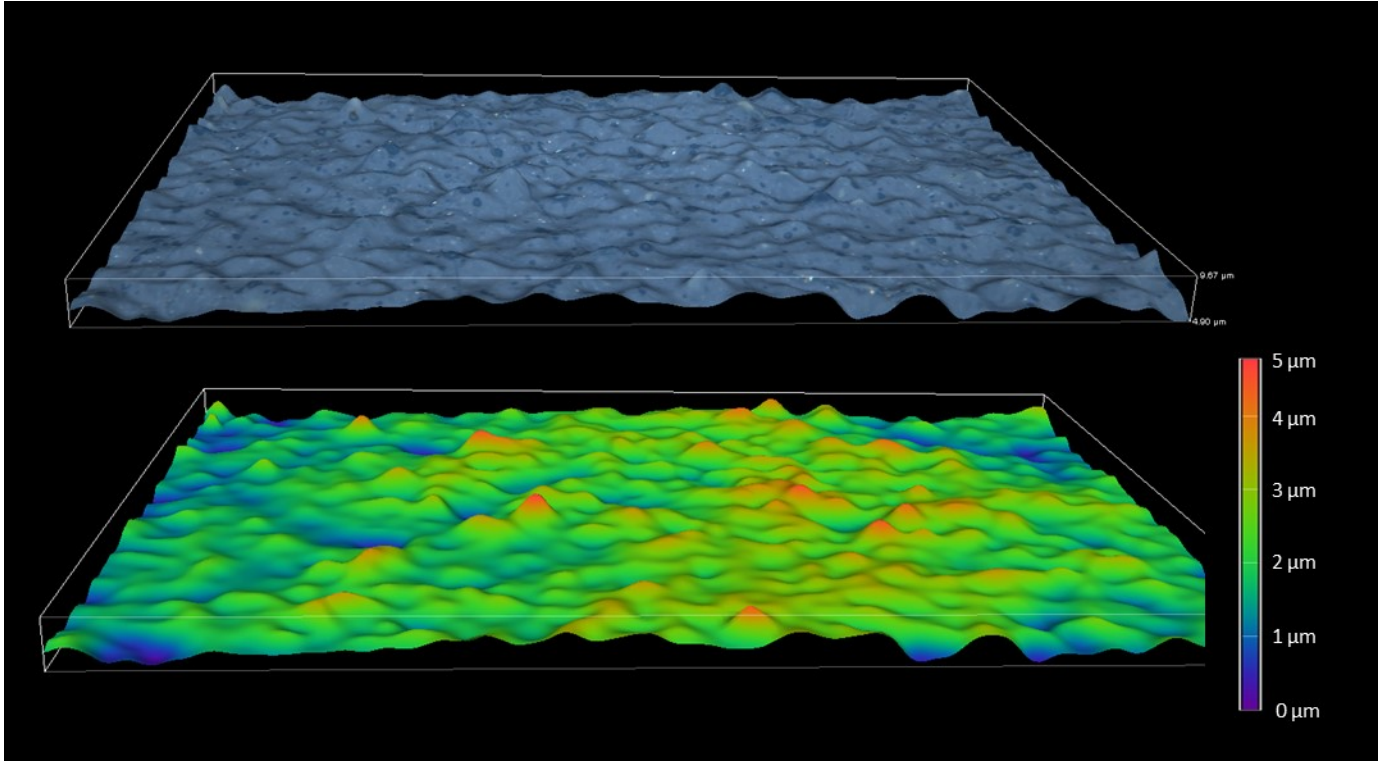


Figure S22. 3D visualization of the microscopy image of Figure S21, highlighting the height profile of the PVC surface.

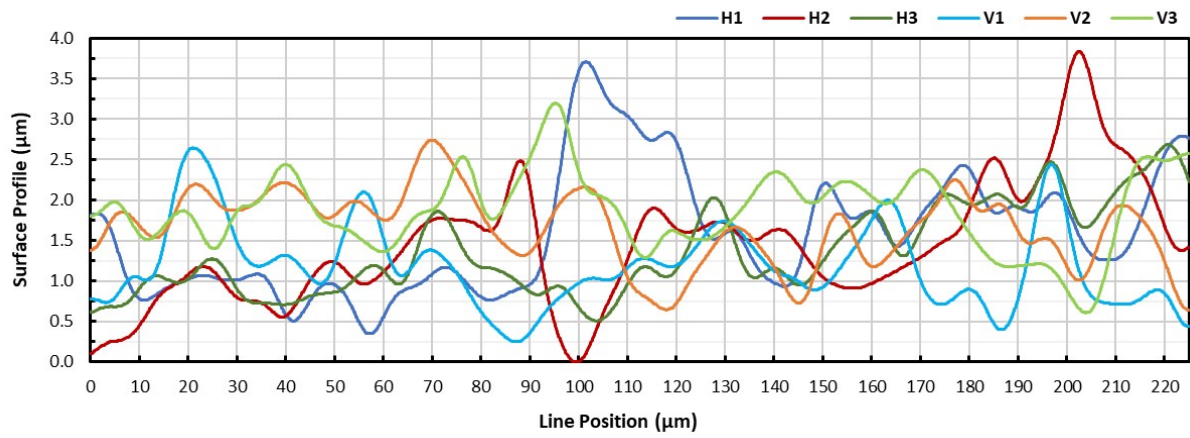


Figure S23. Surface profile of six cross sections of Figure S21 (three sections drawn horizontally in Figure S21, and three sections drawn vertically in Figure S21) that give an outline of the PVC roughness.